the Mach stem near the von Neumann criterion, which makes its numerical resolution very difficult. Figure 3 demonstrates clearly the existence of the flow Mach number variation-induced hysteresis.

Conclusions

It was shown numerically that, in addition to the wedge-angle variation-induced hysteresis in the RR $\leftrightarrow$ MR transition, which was first illustrated numerically in Ref. 10, a flow Mach number variation-induced hysteresis is also possible in two-dimensional steady flows. For the latter, two different shock wave reflection configurations can be obtained at the same values of angle of incidence and flow Mach number, depending on the direction from which the flow Mach number was reached.

Because the investigated geometry resembles the geometry of supersonic intakes, the new hysteresis type that is reported in the present study can be relevant to flight performance at high supersonic speeds. The possible dependence of the flow pattern on the preceding maneuvers of an aircraft should be taken into account in designing intakes for perspective hypersonic vehicles.

Acknowledgment

The Russian authors of this Note would like to acknowledge the support of the Russian Foundation for Basic Research, Grant 00-01-00824.

References

[1]Ben-Dor, G., *Shock Wave Reflection Phenomena*, Springer-Verlag, New York, 1991, Chap. 3.

[2]Von Neumann, J., "Oblique Reflection of Shocks," Navy Dept., Explosive Research Rept. 12, Bureau of Ordnance, Washington, DC, 1943 (reprinted in *Collected Works of J. von Neumann,* Vol. 6, Pergamon, Oxford, 1963, pp. 238–299).

[3]Hornung, H. G., Oertel, H., Jr., and Sandeman, R. J., "Transition to Mach Reflection of Shock Waves in Steady Flow With and Without Relaxation," *Journal of Fluid Mechanics*, Vol. 90, 1979, pp. 541–560.

[4]Hornung, H. G., and Robinson, M. L., "Transition from Regular to Mach Reflection of Shock Waves. Part 2. The Steady Flow Criterion," *Journal of Fluid Mechanics*, Vol. 123, 1982, pp. 155–164.

[5]Henderson, L. F., and Lozzi, A., "Further Experiments on Transition to Mach Reflection," *Journal of Fluid Mechanics,* Vol. 94, 1979, pp. 541–559.

[6]Teshukov, V. M., "On Stability of Regular Reflection of Shock Waves," *Prikladnaya Mekhanika i Technicheskaya Fizika (Applied Mechanics and Technical Physics)*, No. 2, 1989, pp. 26–33 (in Russian).

[7]Li, H., and Ben-Dor, G., "Application of the Principle of Minimum Entropy Production to Shock Wave Reflections. I. Steady Flows," *Journal Applied Physics*, Vol. 80, 1996, pp. 2027–2037.

[8]Chpoun, A., Passerel, D., Li, H., and Ben-Dor, G., "Reconsideration of the Oblique Shock Wave Reflection in Steady Flows. I. Experimental Investigation," *Journal of Fluid Mechanics*, Vol. 301, 1995, pp. 19–35.

[9]Vuillon, J., Zeitoun, D., and Ben-Dor, G., "Reconsideration of the Oblique Shock Wave Reflection in Steady Flows. I. Experimental Investigation," *Journal of Fluid Mechanics*, Vol. 301, 1995, pp. 37–50.

[10]Ivanov, M. S., Gimelshein, S. F., and Beylich, A. E., "Hysteresis Effect in Stationary Reflection of Shock Waves," *Physics of Fluids*, Vol. 7, 1995, pp. 685–687.

[11]Li, H., Chpoun, A., and Ben-Dor, G., "Analytical and Experimental Investigations of the Reflection of Asymmetric Shock Waves in Steady Flow," *Journal of Fluid Mechanics*, Vol. 390, 1999, pp.25–43.

[12]Ben-Dor, G., "Hysteresis Phenomena in Shock Wave Reflections in Steady Flows," *Proceedings of 22nd International Symposium on Shock Waves*, Vol. 1, edited by G. J. Ball, R. Hillier, and G. T. Roberts, Univ. of Southampton, Southampton, England, U.K., 1999, pp. 49–56.

[13]Onofri, M., and Nasuti, F., "Theoretical Considerations on Shock Reflections and Their Implications on the Evaluations of Air Intake Performance," *Proceedings of 22nd International Symposium on Shock Waves*, Vol. 2, edited by G. J. Ball, R. Hillier, and G. T. Roberts, Univ. of Southampton, Southampton, England, U.K., 1999, pp. 1285–1290.

[14]Khotyanovsky, D. V., Kudryavtsev, A. N., and Ivanov, M. S., "Numerical Study of Transition Between Steady Regular and Mach Reflection Caused by Free-Stream Perturbations," *Proceedings of 22nd International Symposium on Shock Waves*, Vol. 2, edited by G. J. Ball, R. Hillier, and G. T. Roberts, Univ. of Southampton, Southampton, England, U.K., 1999, pp. 1261–1266.

P. Givi
Associate Editor

Influence of External Caps on the Dynamic Behavior of Aerospace Cylindrical Vessels

Silvano Tizzi*
University of Rome "La Sapienza," 00184 Rome, Italy

Introduction

A MORE complete structural numerical simulation model than the one utilized in a previous work[1] for the dynamic analysis of cylindrical tanks is necessary for the analysis of the dynamic behavior of vessel structures with axisymmetric caps at the ends, which can be applied to generic axisymmetric shells of revolution.

Flugge[2] introduced a simplified linear model for static and dynamic behavior of axisymmetric thin shells (also see Ref. 3). Narasimhan and Alwar[4] utilized the same model for a study of vibration of orthotropic spherical shells and introduced an interesting numerical procedure based on the Chebyshev–Galerkin spectral method for the evaluation of free vibration frequencies and modal shapes.

Hwang and Foster utilized a similar and simpler model for a study of the dynamic behavior of isotropic shallow spherical shells with a circular hole,[5] but the out-of-plane shear behavior and rotary inertia were not taken into account. They found a solution of the free vibrational frequency equation in terms of Bessel functions and modified Bessels functions.

Ozakca and Hinton[6] built a Mindlin[7]–Reisner[8] axisymmetric finite element model with the same kinematic relations, where the out-of-plane and rotary inertia effects with varying shell thickness are taken into account, for a free vibration analysis and optimization of axisymmetric shells of revolutions.

As in the previous work,[1] a simplified numerical model for the dynamic analysis of an orthotropic antisymmetric angle-ply laminated axisymmetric shell has been developed here. The considered structure is the same as the one dealt with by Mizusava and Kito,[9] who utilized the first-order shear deformation Sanders' shell theory to analyze the vibration behavior. An out-of-plane shear stress distribution along the thickness coordinate according the Mindlin[7]–Reisner[8] theory is imposed. The same kinematic relations utilized by the mentioned authors,[1–5] with appropriate approximations, have been employed to build this structural model.

A numerical procedure,[1,10–13] which lies between the Rayleigh–Ritz method (see Refs. 14 and 15) and the finite element method (FEM)[3,16,17] and which is obtained by combining the Ritz analysis with the variational principles,[18–20] has been applied to find the free frequencies and vibration modes.

We have seen in the whole cylindrical structure case that there are low-frequency (lf) vibrating modes, flexural and flexural–torsional (FT) modes, and high-frequency (hf) shear vibration modes, where the displacements can be neglected with respect to the rotations: These can be divided into shear–flexural (SF) modes, where the rotation ϕ_s is predominant with respect to the rotation ϕ_y, and shear–torsional (ST) modes, where, on the contrary, ϕ_s can be neglected with respect to ϕ_y.

The same vibration modes have been considered here, particularly with regard to the influence of the external axisymmetric caps on them. Finally, the dependence of both lf and hf on the winding angle on the cylindrical central part, which can be an important parameter in the design of the aerospace vehicles vessels, has been considered.

Mathematical Model

A vessel shell profile is considered and a reference system s, y, z_s (Fig. 1), where s and y are oriented along the tangent to the cap

Received 12 April 2000; revision received 5 July 2000; accepted for publication 5 July 2000.

*Researcher, Aerospace Department.

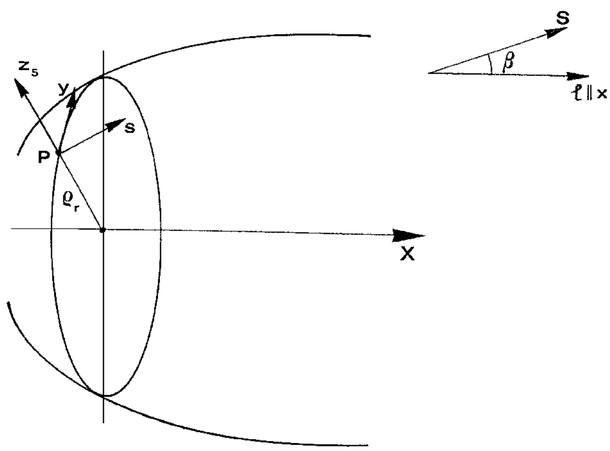

Fig. 1 Axisymmetric cap reference system.

profile and the circular direction, respectively, and z_s is the coordinate along the direction normal to the cap surface. We introduce the nondimensional axial coordinate $\xi = x/L$ and the nondimensional radius of the cylinder $R = r/L$, where L is the vessel structure axial length. Also the radius ρ_r of the cap at the point P can be written in nondimensional form, $\rho_L = \rho_r/L$, together with the meridian curvature radius, $\rho_{ML} = \rho_M/L$ and the tangent meridian coordinate $s_L = s/L$. In the central cylindrical part of the structure, we have $\rho_L = R$, and the cap meridian nondimensional curvature $c_M = 1/\rho_{ML}$ vanishes.

The displacements of a point on the middle surface ($z_s = 0$) u, v, and w along the axes s, y, and z_s, respectively, are then introduced, which can be reformulated in nondimensional form as

$$U = u/L, \qquad V = v/L, \qquad W = w/L \tag{1}$$

together with the rotations ϕ_s and ϕ_y around the axes $-y$ and s, respectively.

The kinematic relations[1–5] can be written as

$$\epsilon_s = \frac{\partial U}{\partial s_L} + \frac{W}{\rho_{ML}} + \frac{z_s}{L}\frac{\partial \phi_s}{\partial s_L}$$

$$\epsilon_y = \frac{\partial V}{\rho_L \partial \theta} + \frac{W\cos(\beta)}{\rho_L} + \frac{U\sin(\beta)}{\rho_L} + \frac{z_s}{L}\left(\frac{\partial \phi_y}{\rho_L \partial \theta} + \frac{\phi_s \sin(\beta)}{\rho_L}\right)$$

$$\gamma_{sy} = \frac{\partial U}{\rho_L \partial \theta} + \frac{\partial V}{\partial s_L} - \frac{V\sin(\beta)}{\rho_L} + \frac{z_s}{L}\left[\frac{\partial \phi_y}{\partial s_L} + \frac{\partial \phi_s}{\rho_L \partial \theta} - \frac{\sin(\beta)\phi_y}{\rho_L}\right]$$

$$\gamma_{sz} = \frac{\partial W}{\partial s_L} - \frac{U}{\rho_{ML}} - \phi_s, \qquad \gamma_{yz} = \frac{\partial W}{\rho_L \partial \theta} - \frac{V\cos(\beta)}{\rho_L} - \phi_y \tag{2}$$

From these it is easy to arrive at the constitutive relations between stress moment and displacement rotation for isotropic axisymmetric thin shells,[21] which can be properly modified for ortotropic structures in composite materials.[9,22,23] They can be written as

$$\{N\} = [A]\left\{\epsilon^{(0)}\right\}, \qquad \{F\} = [D]1/L\left\{\chi^{(\phi)}\right\}, \qquad \{V\} = [G]\{\gamma\} \tag{3}$$

where $\{N\}$, $\{F\}$, and $\{V\}$ are the column vectors of the membrane forces, flexural and torsional moments, and the out-of-plane resulting shear stresses, respectively,

$$\{N\} = \begin{Bmatrix} N_s \\ N_y \\ N_{sy} \end{Bmatrix}, \qquad \{F\} = \begin{Bmatrix} F_s \\ F_y \\ F_{sy} \end{Bmatrix}, \qquad \{V\} = \begin{Bmatrix} V_s \\ V_y \end{Bmatrix} \tag{4}$$

$[A]$, $[D]$, and $[G]$ are the in-plane, out-of-plane, flexural and torsional, and shear rigidity parameters matrices, respectively,

$$[A] = \begin{bmatrix} A_{ss} & A_{sy} & 0 \\ A_{sy} & A_{yy} & \\ 0 & 0 & A_{sh} \end{bmatrix}, \qquad [D] = \begin{bmatrix} D_{ss} & D_{sy} & 0 \\ D_{sy} & D_{yy} & 0 \\ 0 & 0 & D_{sh} \end{bmatrix}$$

$$[G] = \begin{bmatrix} G^*_{sz} & 0 \\ 0 & G^*_{yz} \end{bmatrix} \tag{5}$$

with $G^*_{sz} = G_{sz}/\chi_s$ and $G^*_{yz} = G_{yz}/\chi_y$. Also, $\{\epsilon^{(0)}\}$ is the column vector of the in-plane strain contribution due to the displacements U, V, and W; $\{\chi^{(\phi)}\}$ is the column vector of the bending and twisting curvatures, depending on the rotations ϕ_s and ϕ_y, which multiplied by the nondimensional thickness coordinate z_s/L gives the in-plane strain contribution due to the bending and torsion; and $\{\gamma\}$ is the column vector of the out-of-plane shear strain, as in Eqs. (2),

$$\left\{\epsilon^{(0)}\right\} = \begin{Bmatrix} \dfrac{\partial U}{\partial s_L} + \dfrac{W}{\rho_{ML}} \\ \dfrac{\partial V}{\rho_L \partial \theta} + \dfrac{W\cos(\beta)}{\rho_L} + \dfrac{U\sin(\beta)}{\rho_L} \\ \dfrac{\partial U}{\rho_L \partial \theta} + \dfrac{\partial V}{\partial s_L} - \dfrac{V\sin(\beta)}{\rho_L} \end{Bmatrix}$$

$$\left\{\chi^{(\phi)}\right\} = \begin{Bmatrix} \dfrac{\partial \phi_s}{\partial s_L} \\ \dfrac{\partial \phi_y}{\rho_L \partial \theta} + \dfrac{\phi_s \sin(\beta)}{\rho_L} \\ \dfrac{\partial \phi_s}{\rho_L \partial \theta} + \dfrac{\partial \phi_y}{\partial s_L} - \dfrac{\phi_y \sin(\beta)}{\rho_L} \end{Bmatrix}$$

$$\{\gamma\} = \begin{Bmatrix} \dfrac{\partial W}{\partial s_L} - \dfrac{U}{\rho_{ML}} - \phi_s \\ \dfrac{\partial W}{\rho_L \partial \theta} - \dfrac{V\cos(\beta)}{\rho_L} - \phi_y \end{Bmatrix} \tag{6}$$

All of the introduced elastic rigidity parameters of the shell structure have been determined by the composite laminate theory,[1,9,22,23] once the single-layer elastic proporties are known, as in the previous model.[1]

Because the laminate is characterized by an high number of layers, with couples of laminas oriented at $\pm\alpha$, balanced and symmetric hypotheses can be approximately satisfied, for which there is uncoupling between in-plane and out-of-plane behaviors. The rigidity parameters matrix $[B]$, connecting them,[22,23] can be neglected.

Consequently, the total strain energy expression can be written as

$$\mathcal{E}_T = \frac{1}{2}\int_S \left\{\left[\epsilon^{(0)}\right]_T[\boldsymbol{A}]\left[\epsilon^{(0)}\right] + \frac{1}{L^2}\left[\chi^{(\phi)}\right]_T[\boldsymbol{D}]\left[\chi^{(\phi)}\right] + [\gamma]_T[\boldsymbol{G}][\gamma]\right\} \mathrm{d}S \tag{7}$$

which can be expressed vs the displacements and rotations taking into account the kinematic relations in Eqs. (2).

The kinetic energy expression is

$$\mathcal{T} = \frac{1}{2}\omega^2 L^2 h \int_S \rho(U^2 + V^2 + W^2)\,\mathrm{d}S + \frac{1}{2}\omega^2 \int_S J\left(\theta_x^2 + \theta_\theta^2\right)\mathrm{d}S \tag{8}$$

where $J = \rho h^3/12$ is the inertia moment per unity surface. In the numerical approach, the axisymmetric structure is divided into N_E elements along the axial direction. For the generic variable $Q(\xi, \theta)$ (which can be U, V, and W or the rotations ϕ_s and ϕ_y), we choose a series expansion of hybrid describing functions[1,4,24,25] in the generic lth element, both global and local[1,13]:

$$Q(\xi, \theta) = \left[\sum_{i=1}^{N_g} q_i \xi^i (1-\xi) + \sum_{ie=1}^{N_l} q_{ie}^{(l)} \xi_e^{ie}(1-\xi_e)\right] \times \sin(m\theta) \quad \text{or} \quad \cos(m\theta) \tag{9}$$

where

$$l = 1, 2, \ldots, N_E, \qquad \xi_l = l/N_E, \qquad \xi_{l-1} \le \xi \le \xi_l$$

$$\xi_e = (\xi - \xi_{l-1})N_E, \qquad 0 \le \xi_e \le 1 \tag{9'}$$

and ξ_e is the normalized nondimensional axial coordinate of the considered component element, N_g is the number of the global describing functions defined throughout the whole vessel structure, and N_l is the number of the local describing functions defined in each single component element, which vanish at the borders of the same so that the continuity of the resultant function is not lost.

If we choose $\cos(m\theta)$ for the circular behavior of U, W, and ϕ_s, the corresponding behavior function of V and ϕ_y must be $\sin(m\theta)$ or vice versa. The first choice is obliged if $m = 0$, when it is considered that in such a case of axisymmetric vibrating mode the variables V and ϕ_y vanish.

If the series expansions (9) are substituted into Eqs. (7) and (8), it is possible to know the expressions of the strain and kinetic energy vs the Lagrangian degrees of freedom, which are the coefficients of the series expansions q_i and q_{i_e}. Thus, the stiffness and mass matrices can be formed. By imposing the stationary conditions of the total energy Lagrangian functional,[19,20] we arrive at the generalized eigenvalue problem, the solution of which is found by the algorithm F02BJF of the NAG utility package.[26] (It is a mathematical library with numerical programs to solve many computational problems.)

Application

A particular case of laminate with 20 helicoidal layers of the cylindrical skin structure will be considered. The geometric characteristics referring to the central cylindrical part are shown in Fig. 2. The elasticity parameters, referring to the single-layer reference system x_1, x_2 are defined as follows:

$$E_1 = 130 \text{ GPa}, \qquad E_2 = 6.9 \text{ GPa}, \qquad \nu_{12} = 0.27$$

$$g_{12} = 4.48 \text{ GPa}, \qquad g_{1z} = 8.9 \text{ GPa}, \qquad g_{2z} = g_{12}$$

$$\chi_x = \tfrac{5}{6}, \qquad \chi_y = \tfrac{5}{6}$$

and $L = 250$ mm is the tank length, as in the previous case of the whole cylindrical structure.[1]

The characteristics of the end caps are very similar to the ones utilized in most practical applications. For the cap at the first left end, a circumferential radius behavior vs the normalized nondimensional axial coordinate $\xi^{(1)}$ is supposed to be

$$\rho_L\left(\xi^{(1)}\right) = \left\{1 + t_{r1}\left(\xi^{(1)} + 0.01\right)^{0.5} - 0.9 - 0.5t_{r1}1.01^{-0.5}\xi^{(1)}\right\}R \tag{10}$$

$$\xi^{(1)} = 10\xi, \qquad t_{r1} = 0.9(2 \times 1.01^{0.5}/1.02) \tag{10'}$$

and a winding angle α is supposed as

$$\alpha = \left[1 - \exp\left(-24c_{pr}^{1.8}\right)\right]\alpha_c \tag{11}$$

$$c_{pr} = \xi^{(1)}/0.2 \qquad \text{for} \qquad \xi^{(1)} \le 0.2 \tag{11'}$$

$$\alpha = \{1 - 0.2[(c_{m2}/0.8) - 1](c_{m2}/0.8)\}\alpha_c \tag{12}$$

$$c_{m2} = \xi^{(1)} - 0.2 \qquad \text{for} \qquad \xi^{(1)} > 0.2 \tag{12'}$$

The corresponding values vs ξ are shown in Table 1, together with those of angle β between the meridian tangent and the vessel axis, $\beta = \tan^{-1}(\mathrm{d}\rho_L/\mathrm{d}\xi)$.

At the right end cap, we have

$$\rho_L\left(\xi^{(2)}\right) = \left[1 + t_{r1}\left(1.5 - \xi^{(2)}\right)^{0.5} - 4.1 - t_{r1}\Big/\left(2 \times 1.5^{0.5}\right) + t_{r1}\xi^{(2)}\Big/\left(2 \times 1.5^{0.5}\right)\right]R \tag{13}$$

$$\xi^{(2)} = 10(\xi - 0.9), \qquad t_{r1} = 4.1(2 \times 1.5^{0.5})/2 \tag{13'}$$

$$\alpha = \left\{1 - \exp\left(-30 \times \left[1 - \xi^{(2)}\right]^{1.75}\right)\right\}\alpha_c \tag{14}$$

The values of the same parameters and also those of angle β vs the axial coordinate of the right end cap are reported in Table 2.

Results

The obtained results, when not specified, refer to the case with the winding angle $\alpha_c = 18$ deg. The values of the nondimensional frequency parameter ω_p, which is connected with the true frequency ω via the following relation:

$$\omega_p^2 = \omega^2 \rho L^2 \Big/ E_0 \tag{15}$$

where $E_0 = 1$ GPa is a reference Young modulus, are considered.

Table 1 Values of ρ, α, and β vs ξ and $\xi^{(1)}$ at the left end cap

ξ	$\xi^{(1)}$	ρ_L	α	β
0.0000	0.0000	0.0501	0.0000	1.5016
0.0100	0.1000	0.1084	0.3138	1.2712
0.0200	0.2000	0.1330	0.3142	1.0868
0.0300	0.3000	0.1487	0.3210	0.9089
0.0400	0.4000	0.1595	0.3259	0.7373
0.0500	0.5000	0.1672	0.3289	0.5759
0.0600	0.6000	0.1727	0.3299	0.4288
0.0700	0.7000	0.1765	0.3289	0.2981
0.0800	0.8000	0.1789	0.3259	0.1839
0.0900	0.9000	0.1803	0.3210	0.0851
0.1000	1.0000	0.1807	0.3142	0.0000

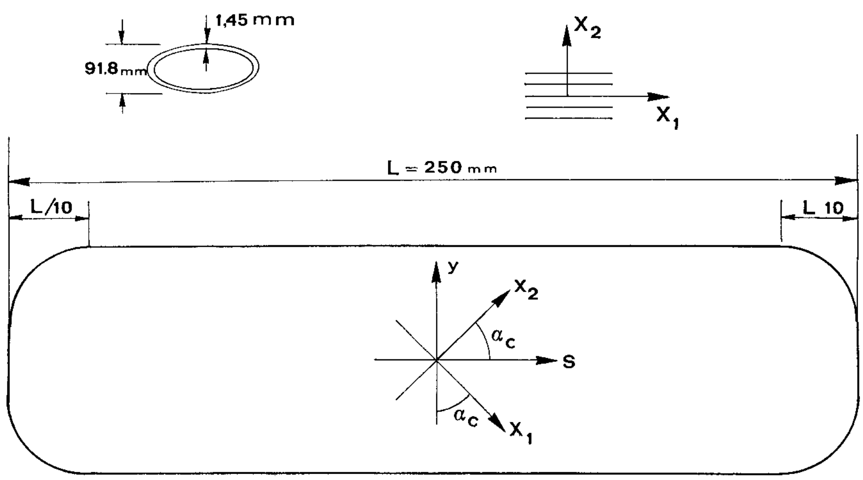

Fig. 2 Geometry of a vessel structure.

Table 2 Values of ρ, α, and β vs ξ and $\xi^{(2)}$ at the right end cap

ξ	$\xi^{(2)}$	ρ_L	α	β
0.9000	0.0000	0.1807	0.3142	0.0000
0.9100	0.1000	0.1801	0.3142	−0.1293
0.9200	0.2000	0.1781	0.3142	−0.2681
0.9300	0.3000	0.1745	0.3142	−0.4122
0.9400	0.4000	0.1692	0.3142	−0.5560
0.9500	0.5000	0.1620	0.3141	−0.6943
0.9600	0.6000	0.1525	0.3134	−0.8229
0.9700	0.7000	0.1403	0.3060	−0.9396
0.9800	0.8000	0.1249	0.2619	−1.0437
0.9900	0.9000	0.1056	0.1299	−1.1359
1.0000	1.0000	0.0814	0.0000	−1.2175

Table 3 Flexural lf ($m = 0$) obtained with and without caps

	Caps			Cylindrical
Mode	$N = 235$	$N = 240$	$N = 245$	$N = 170$
First	3.612	3.612	3.611	8.592
Second	10.148	10.140	10.140	17.079
Third	17.650	17.650	17.650	25.319
Fourth	24.378	24.372	24.372	33.029
Fifth	29.494	29.490	29.490	39.746

Table 4 Relative divergence between the natural frequencies of the structure with and without the end caps

	Flexural	FT		Torsional
Mode	$m = 0$	$m = 1$	$m = 2$	$m = 0$
First	0.580	0.456	0.280	0.552
Second	0.406	0.248	0.158	0.385
Third	0.303	0.211	0.048	0.272
Fourth	0.262	0.180	−0.008	0.206
Fifth	0.258	0.206	−0.027	0.167

The flexural lf ($m = 0$) are shown in Table 3, in the caps columns, when the external caps presence is considered, whereas, if the whole structure is supposed cylindrical, the values have been already determined in the previous work.[1]

The best choice of N_E and N_l is $N_E = 10$ and $N_l = 4$. Consequently, if we recall the expression of the total number of Lagrangian degrees of freedom[1]:

$$N = 5N_E N_l + 5N_g \tag{16}$$

because the number N_g of global describing functions varies from 7 to 10, N lies between 235 and 250. The results obtained with higher values of N_g are not more reliable.

The obtained values of the hf, SF and ST, have not been reported because they are nearly coincident with the corresponding ones obtained in the whole cylindrical structure case.[1]

An important parameter of this study is the relative divergence between the natural frequencies of the structure with, ω_{caps}, and without, ω_{cyl}, the end caps, that is,

$$\Delta\omega/\omega_{\text{cyl}} = (\omega_{\text{cyl}} - \omega_{\text{caps}})/\omega_{\text{cyl}} \tag{17}$$

In Table 4, these mentioned parameter values for the lf, flexural ($m = 0$), FT ($m = 1$ and 2), and torsional ($m = 0$) are reported, when the winding angle α_c in the central cylindrical part is 18 deg.

The dependence of the same parameter vs the order mode identification number $n^{(\text{mode})}$ (where 1 corresponds to First, 2 corresponds to Second, etc.) considered as a continuous variable is shown in Fig. 3 for the flexural modes ($m = 0$) and the FT modes ($m = 1$, and 2).

The modal shapes have to be considered, too, even if they have not been reported in the text. Note that in the hf range the SF and ST

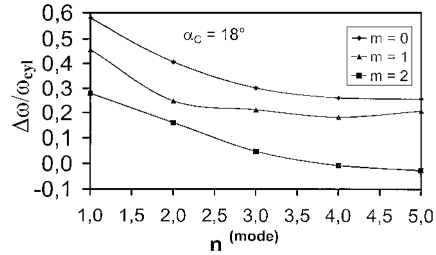

Fig. 3 Behavior of the lf, flexural ($m = 0$) and FT ($m = 1$ and 2), relative divergence vs order mode identificative number $n^{(\text{mode})}$ for $\alpha_c = 18$ deg.

vibrating modes are uncoupled, as in the previous case of cylindrical structure without caps. Consequently, in the SF mode, the rotation ϕ_y is negligible with respect to ϕ_s, whereas in the ST modes, ϕ_s is negligible with respect to ϕ_y.

There is some difference between the lf modes, flexural and FT, obtained here, and the corresponding ones of the whole cylindrical structure case, particularly at the boundaries between the caps and the central body.

The behaviors of the lf torsional modes and of the hf modal shapes, SF and ST, are very similar to the ones of the whole vessel cylindrical structure case.[1]

Discussion

From the results obtained, it is evident that both the complexity of the vibration modes and the winding angle α_c diminishes the relative divergence between the frequencies of the cylindrical structure, with and without the caps.

From Fig. 3 note that the divergence diminishes with the mode order number $n^{(\text{mode})}$ and that for $m = 2$ (and over) it becomes very small as $n^{(\text{mode})}$ increases indefinitely, whereas for $m = 0$ and 1, there is a trend to stabilize, but with a lower value for $m = 1$ than for $m = 0$.

It is possible to observe that for the flexural vibration modes ($m = 0$) the divergence parameter decreases with $n^{(\text{mode})}$ more and more as the winding angle α_c grows, if we look at its behavior vs $n^{(\text{mode})}$ for different values of α_c, which has not been reported in the text. Also in the case of torsional modes ($m = 0$), the same parameter decreases vs $n^{(\text{mode})}$.

Note that the divergence of the hf, SF and ST, in the two cases, with and without caps, is nearly nonexistent.

Also, with end caps presence there is the possibility of the discontinuity of the independent variables first derivative in their modal function. In effect this can be seen by looking at the axial displacement U behavior at the boundaries between the end caps and the central cylindrical part of the FT ($m = 1, 2$) modal shapes, which has not been reported in the text.

Conclusions

We have seen that, if we consider the flexural and FT modes, for $\alpha_c = 18$ deg, the relative divergence is small if $n^{(\text{mode})} \geq 3$ and $m \geq 2$. For high values of the winding angle α_c, such divergence becomes negligible from $m = 0$ and over if $n^{(\text{mode})} \geq 3$.

Consequently, in such cases it is possible to obtain flexural and FT eigensolutions with a good approximation with the old model of the cylindrical structure without end caps, which is much simpler, allows saving a lot of Lagrangian degrees of freedom, and avoids complicated numerical operations. This is particularly true for hf, which are nearly coincident in the two cases considered.

The introduction of local describing functions, defined in each single structural component element, which in the previous case of cylindrical vessel was useful to obtain more accurate results and a better convergence rate, is mandatory in this caps case for the FT modes because only with these is it possible to develop a discontinuity presence of the axial displacement first derivative at the boundaries between caps and central tank body, if the internal border of each cap lies on the edge between two adjacent elements. Note that within each element the resultant describing function is perfectly continuous and regular.

However, this particular sophisticated model utilized for the dynamic analysis of aerospace vehicles vessels with end caps, although having complicated numerical operations, offers accurate frequency results to be obtained with an high convergence rate.

References

[1]Tizzi, S., "Free Frequencies and Modal Shapes of Cylindrical Vibrating Composite Structures," *Computers and Structures*, Vol. 73, No. 6, 1999, pp. 629–653.

[2]Flugge, W., *Stresses in Shells*, Springer-Verlag, Berlin, 1962, pp. 312–371.

[3]Brebbia, C. A., and Connor, J. J., *Fondamenti del Metodo degli Elementi Finiti*, Clup, Milan, 1978, pp. 218–224.

[4]Narasimham, M. C., and Alwar, R. S., "Free Vibration Analysis of Laminated Orthotropic Spherical Shells," *Journal of Sound and Vibration*, Vol. 154, No. 3, 1992, pp. 515–529.

[5]Hwang, D. Y., and Foster, W. A., Jr., "Analysis of Axisymmetric Free Vibration of Isotropic Shallow Spherical Shells with a Circular Hole," *Journal of Sound and Vibration*, Vol. 157, No. 2, 1992, pp. 331–343.

[6]Ozakca, M., and Hinton, E., "Free Vibration Analysis and Optimization of Axisymmetric Plates and Shells—I. Finite Element Formulation," *Computers and Structures*, Vol. 52, No. 6, 1994, pp. 1181–1197.

[7]Mindlin, R. D., "Influence of Rotary Inertia and Shear on Flexural Motions of Isotropic, Elastic Plates," *Journal of Applied Mechanics*, Vol. 18, No. 1, 1951, pp. 31–38.

[8]Reissner, E., "The Effect of Transverse Shear Deformation on the Bending of Elastic Plates," *Journal of Applied Mechanics*, Vol. 12, No. 2, 1945, pp. A69–A77.

[9]Mizusawa, T., and Kito, H., "Vibration of Antisymmetric Angle-Ply Laminated Cylindrical Panels by the Spline Strip Method," *Computers and Structures*, Vol. 56, No. 4, pp. 589–604.

[10]Jaunky, N., Knight, N. F., Jr., and Ambur, D. R., "Buckling of Arbitrary Quadrilateral Anisotropic Plates," *AIAA Journal*, Vol. 33, No. 5, 1995, pp. 938–944.

[11]Tizzi S. "Application of a Numerical Procedure for the Dynamic Analysis of Plane Aeronautical Structures," *Journal of Sound and Vibration*, Vol. 193, No. 5, 1996, pp. 957–983.

[12]Tizzi, S., "Numerical Procedure for the Dynamics Analysis of Three Dimensional Aeronautical Structures," *Journal of Aircraft*, Vol. 34, No. 1, 1997, pp. 120–130.

[13]Tizzi, S., "Improvement of a Numerical Procedure for the Dynamic Analysis of Aircraft Structures," *Journal of Aicraft*, Vol. 37, No. 1, 2000, pp. 144–154.

[14]Kantorovich, L. V., and Krylov, V. I., *Approximate Methods of Higher Analysis*, Interscience, New York, 1964, pp. 258–303.

[15]Reddy, J. N., *Applied Functional Analysis and Variational Methods in Engineering*, McGraw–Hill, New York, 1986, pp. 258–285.

[16]Hughes, T. J. R., *The Finite Elements Method, Linear Static and Dynamic Finite Element Analysis,* Prentice–Hall, Upper Saddle River, NJ, 1987, pp. 383–417.

[17]Reddy, J. N., Krishnamoorthy, C. S., and Seetharamu, K. N., *Finite Element Analysis for Engineering Design*, Springer-Verlag, Berlin, 1988, pp. 361–425.

[18]Mikhlin, S. G., *Variational Methods in Mathematical Physics*, Pergamon, Oxford, 1964, pp. 74–125.

[19]Pars, L. A., *A Treatise of Analytical Dynamics*, Heinemann, London, 1968, pp. 34–37.

[20]Fichera, G., *Numerical and Quantitative Analysis*, Pitman, London, 1978, pp. 1–12.

[21]Santini, P., *Introduzione alla Teoria delle Strutture*, Tamburini Editore, Milan, 1973, pp. 437–438.

[22]Gibson, R. F., *Principles of Composite Material Mechanics*, McGraw–Hill, New York, 1994, Chaps. 2, 7.

[23]Marchetti, M., and Cutolo, D., *Tecnologie dei Materiali Compositi*, Editoriale ESA, Milan, 1987, pp. 36–38, 55–63.

[24]Swaddiwudhipong, S., Tian, J., and Wang, C. M., "Vibrations of Cylindrical Shells with Intermediate Supports," *Journal of Sound and Vibration*, Vol. 187, No. 1, 1995, pp. 69–93.

[25]Sivadas, K. R., and Ganesan, N., "Dynamic Analysis of Circular Cylindrical Shells with Material Damping," *Journal of Sound and Vibration*, Vol. 166, No. 1, 1993, pp. 103–116.

[26]"The NAG Fortran Library Manual," Mark 17, Natural Algorithms Group, Inc., Downers Grove, IL, 1995.

A. N. Palazotto
Associate Editor

Classical Normal Modes in Nonviscously Damped Linear Systems

Sondipon Adhiakri*
University of Cambridge, Cambridge, England CB2 1PZ, United Kingdom

Nomenclature

$\boldsymbol{C}$	=	viscous damping matrix
$\mathcal{G}(t)$	=	damping function in the time domain
$\boldsymbol{I}_N$	=	identity matrix of size N
$\boldsymbol{K}$	=	stiffness matrix
$\boldsymbol{M}$	=	mass matrix
N	=	degrees of freedom of the system
$\mathbb{R}$	=	space of real numbers
t	=	time
$\boldsymbol{U}, \boldsymbol{V}$	=	matrices of the right and left eigenvectors
$\mathbf{u}(t)$	=	generalized coordinates
α_i	=	set of real scalars
$\delta(t)$	=	Dirac-delta function
μ_1, μ_2	=	parameters of the GHM[5] damping model

Superscripts

$\bullet^T$	=	matrix transposition of $\bullet$
$\bullet^{-T}$	=	inversed transpose of $\bullet$
$\bullet^{-1}$	=	matrix inversion of $\bullet$
$\dot{\bullet}$	=	differentiation of $\bullet$ with respect to t

Introduction

IN general, dynamic systems are nonviscously damped. Possibly the most general way to model damping within the linear range is to consider nonviscous damping models that depend on the past history of motion via convolution integrals over some kernel functions. The equations of motion describing free vibration of an N-degree-of-freedom linear system with such damping can be expressed by

$$\boldsymbol{M}\ddot{\mathbf{u}}(t) + \int_{-\infty}^{t} \mathcal{G}(t-\tau)\dot{\mathbf{u}}(\tau)\,\mathrm{d}\tau + \boldsymbol{K}\mathbf{u}(t) = \mathbf{0} \tag{1}$$

where $\boldsymbol{M}, \boldsymbol{K}, \mathcal{G}(t) \in \mathbb{R}^{N\times N}$. In the special case when $\mathcal{G}(t-\tau) = \boldsymbol{C}\delta(t-\tau)$, Eq. (1) reduces to the case of viscously damped systems. A damping model of this kind is a further generalization of the familiar viscous damping. It is well known that under certain conditions viscously damped symmetric systems possess classical normal modes, that is, $\boldsymbol{M}$, $\boldsymbol{K}$, and $\boldsymbol{C}$ can be diagonalized simultaneously by a real congruence transformation. The most common example in this regard is proportional damping, where the viscous damping matrix has the special form

$$\boldsymbol{C} = \alpha_1\boldsymbol{M} + \alpha_2\boldsymbol{K}, \qquad \alpha_1, \alpha_2 \in \mathbb{R} \tag{2}$$

This damping model is also known as Rayleigh damping or classical damping. Caughey and O'Kelly[1] have proved that viscously damped linear systems with symmetric coefficient matrices possess classical normal modes if, and only if, the relationship

$$\boldsymbol{K}\boldsymbol{M}^{-1}\boldsymbol{C} = \boldsymbol{C}\boldsymbol{M}^{-1}\boldsymbol{K} \tag{3}$$

is satisfied. Based on this result, they have shown that the series representation of damping

Received 18 August 2000; revision received 30 December 2000; accepted for publication 20 January 2001.

*Research Associate, Department of Engineering, Trumpington Street; sa225@eng.cam.ac.uk.